International Journal of Environmental Monitoring and Analysis
2024, Vol. 12, No. 4, pp. 74-87
https://doi.org/10.11648/j.ijema.20241204.12

Research Article

Characteristics of Sand-Driving Wind Regime and Sand Drift Potential in Sandy Areas on Both Sides of Longyangxia Reservoir in China

Lechun Zhang[1], Dengshan Zhang[2, *], Guoyuan Xu[3], Fengling Dong[4], Wanbing Tuo[5]

[1]School of Geological Engineering, Qinghai University, Xining, China
[2]Academy of Agriculture and Forestry Sciences, Qinghai University, Xining, China
[3]Meteorological Information Center of Qinghai Province, Xining, China
[4]Geomatics Technology and Application Key Laboratory of Qinghai Province, Xining, China
[5]College of Engineering, Qinghai Institute of Technology, Xining, China

Abstract

This study focuses on the desertification areas of Talatan and Mugetan, located on both sides of the Longyangxia Reservoir in Qinghai Province, China. These areas pose serious threats to the safety of the reservoir due to frequent wind-sand activities. The research aims to provide a scientific basis for effective sand control by deeply analyzing the dynamic change of wind.The wind speed and direction data from Shazhuyu and Guinan meteorological stations in Qinghai Province, China were used to calculate the numerical and directional characteristics of sand-driving wind and sand drift potential.The results indicate that: (1) The number of sand-driving wind at Talatan is about 7 times that at Mugetan, and the maximum and average wind speeds are about 7 m/s larger than those at Mugetan. At Talatan, the primary sand-driving wind direction is exclusively West Northwest (WNW). Conversely, at Mugetan, the sand-driving wind direction remains westward in spring, autumn, and winter, shifting eastward solely in summer. (2) The annual sand drift potential of Talatan and Mugetan is less than 200VU, two sandy areas are both in low wind energy environments; (3) The major causes of the significant differences in sand-driving wind regimes between the Talatan and Mugetan are topography, precipitation, wind direction stability.These conclusions offer valuable insights for developing targeted sand control strategies, thereby mitigating the potential hazards posed by wind-sand activities to the Longyangxia Reservoir and its surrounding ecosystems.

Keywords

Sand-Driving Wind, Sand Drift Potential, Wind Regime, The Longyangxia Reservoir

*Corresponding author: dshzhang2008@sina.com (Dengshan Zhang)

Received: 25 June 2024; **Accepted:** 23 July 2024; **Published:** 15 August 2024

1. Introduction

The Longyangxia Reservoir is located at the Longyang Gorge, the junction of Gonghe County and Guinan County in Qinghai Province, China, upstream of the Yellow River, with a water storage area of 383 km^2 and a total storage capacity of 24.7 billion m^3, it is currently the largest multi-year regulating reservoir, playing a significant role in governing Yellow River disasters, preventing soil erosion, and driving economic development in Qinghai Province. On both sides of the Longyangxia Reservoir, there are vast sandy areas distributed in the Talatan and Mugetan. From 1987 to 2014, many scholars [1-7] studied the distribution and changes of desertified land on both sides of the reservoir, pointing out that the desertified land on both sides of the reservoir has experienced a process of first deterioration and then partial improvement. Over the years, the wind and sand on both sides of the reservoir have seriously threatened the production and life of local farmers and herdsmen. Instances of roads and houses being buried by sand have been reported. On the other hand, the average amount of wind and sand entering the reservoir directly from the 50-kilometer-long northwest bank sand area is approximately 14.1 million m^3 each year. The collapse of the bank in the reservoir area produces about 21 million m^3 of sediment each year. Over the years, the accumulated sediment entering the reservoir has gradually reduced the capacity of the reservoir, causing considerable losses to the power generation, regulation, flood control, irrigation, and other functions of the reservoir [8, 9].

The characteristics of wind regime and sand drift potential, as standards for measuring the intensity of regional wind-sand activities and evaluating the wind-sand environment, have been discussed by many scholars [10-12] Numerous scholars have also studied the wind regime and sand drift potential characteristics of various landform types in China, such as the Taklimakan Desert [13, 14], Badain Jaran Desert [15], Mu Us Sandy Land [16, 17], Wulanbuhe Desert [18, 19] and other regions; the Qaidam Basin [20], Ruoergai Basin [21], Gonghe Basin [22, 23] and other regions; desertification areas such as the desertification region in northern Shanxi [24] and the Yardan landform region in Guazhou, Gansu Province [25]; lakeshore sand areas such as the eastern part of Qinghai Lake [26] and the basic wind regime and sand drift potential of the other desert areas worldwide [27-30], all of these studies have used wind regime and sand drift potential to measure regional wind-sand activities. However, there is limited research on wind regime and sand drift potential in the sandy areas on both sides of reservoirs. This research deeply explores the sand-driving wind regime and sand drift potential in the sandy areas on both sides of the Longyangxia Reservoir, and comprehensively assesses the wind and sand movement as well as wind energy environment in this area. It not only helps us better understand the laws of wind and sand activities in the sandy areas on both sides of the reservoir, but also provides important scientific basis for managing the sandy areas and preventing wind and sand from entering the reservoir. It is of great theoretical and practical significance for protecting the ecological environment, ensuring the safe operation, and safeguarding the normal function of the reservoir.

2. Materials and Methods

2.1. Overview of the Study Area

The Longyangxia Reservoir is located between 35°19′52″ and 36°33′19″ North Latitude, and 100°12′02″ and 101°29′34″ East Longitude. It runs approximately in a southwest to northeast direction, with a total length of approximately 106km and an average width of 4km. The controlled watershed area is approximately 131,400km^2, and the elevation of the reservoir area ranges from 2,500 to 3,600m. The sandy areas on both sides of the Longyangxia Reservoir are mainly composed of two parts. One is the Talatan Sandy Area, which is located on the northwest side of the reservoir and belongs to Gonghe County. Talatan is situated between the Qinghai Nanshan and Heka Mountains, covering an area of 2,958km^2 and involving six townships: Tiegai, Shazhuyu, Qiabuqia, Tanggemu, Longyangxia, and Niandi. In 2013, the severely desertified area of Talatan was 558km^2, with an intensely developing desertified area of 116km^2, accounting for 23% of the total area. The other part is the Mugetan Sandy Area on the southeast side of the reservoir, which belongs to Guinan County. Mugetan is situated in the southeastern part of the Gonghe Basin, surrounded by the Lajishan, Xiqingshan Mountains, and the Longyangxia Reservoir. The closest part of the Mugetan Sandy Area to the reservoir is only 16km away, with the farthest part, Huangshatou, being about 60km from the reservoir. In 1996, the area of Mugetan was 946km^2, and by 2022, approximately 260km^2 of desert had been treated. Both the Talatan and Mugetan Sandy Areas have relatively flat terrain, with vegetation dominated by arid and semi-arid temperate desert steppe, resulting in low vegetation coverage. The geomorphology of the sandy areas on both sides of the reservoir is shown in Figure 1 below.

2.2. Data Sources

Wind speed, wind direction, and precipitation data were obtained from the Qinghai Provincial Meteorological Information Center. Hourly wind speed and wind direction data from the Shazhuyu and Guinan meteorological stations from June 2019 to May 2022 were processed to calculate the average, maximum values, frequency, and sand drift potential for each month and wind direction. Both stations are national meteorological stations with wind cups installed at a height of 10 meters. As shown in Figure 1, the Shazhuyu meteorological station is located in the heart of the Talatan Sandy Area, while the Guinan meteorological station is located close to the

edge of the Mugetan Sandy Area, only 33 kilometers away from the farthest point of the sandy area known as Huangshatou.

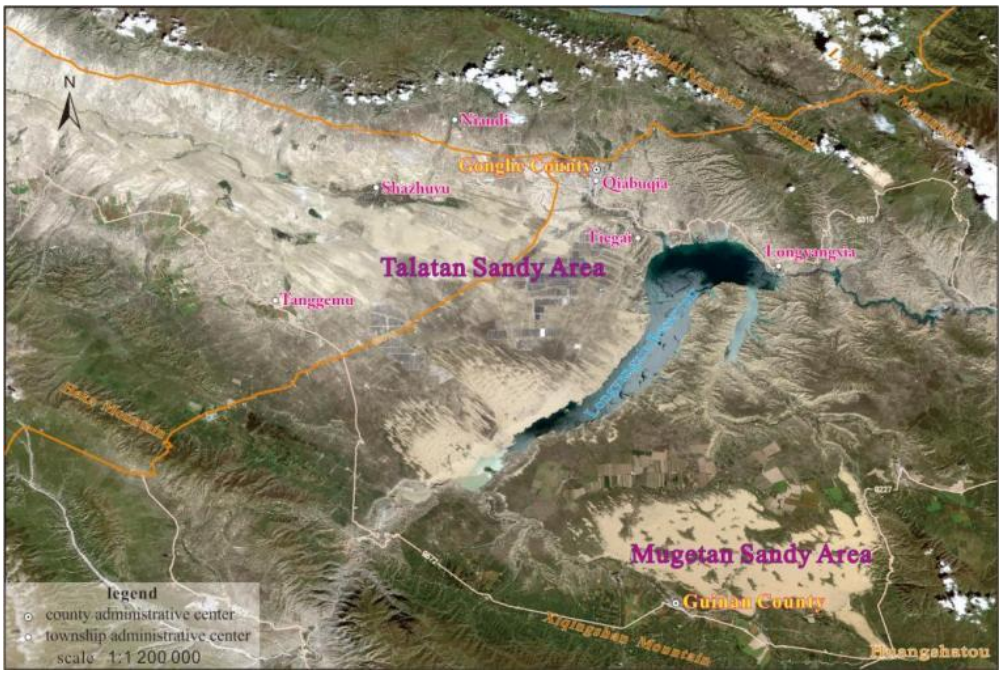

Figure 1. *Topographic map of the sandy areas on both sides of Longyangxia Reservoir.*

2.3. Research Methods

2.3.1. Sand-Driving Wind Regime

As the sandy areas on both sides of the Longyangxia Reservoir are located within the Gonghe Basin, this study adopts a critical sand-driving wind speed of 6m/s based on the research findings of Chen Zongyan et al. [22, 23] regarding sand-driving wind and land desertification in the Gonghe Basin. By analyzing the frequency and wind speed of sand-driving wind in 16 directions (N, NNE, NE, ENE, E, ESE, SE, SSE, S, SSW, SW, WSW, W, WNW, NW, and NNW) for each season of each year, the distribution characteristics of sand-driving wind are examined.

2.3.2. Sand Drift Potential (DP)

FRYBERGER defined the relative potential sand transport rate during a specific period as the sand drift potential (DP) and proposed a formula to calculate it:

$$DP = V^2 * (V - V_t) * t \quad (1)$$

In this formula, DP represents the sand drift potential, with units of vector units (VU); V is the wind speed during sand-driving events; Vt is the critical sand-driving wind speed; and t is the ratio of sand-driving wind time to the observation period (expressed as a percentage, with the observation period typically being one year). While calculating DP according to formula (1) requires the duration of each sand-driving wind event, which is difficult to obtain in practical work, FRYBERGER provided an alternative simplified formula [30] that has also been used by many scholars [31, 32].

$$DP = \sum_{i=1}^{n} V_i^2 * (V_i - V_t) * t_i \quad (2)$$

In this formula, Vi is the wind speed of each sand-driving wind event; Vt is the critical sand-driving wind speed; and ti is the relative frequency of sand-driving wind. Since the data for sand-driving wind in this study are measured in m/s, the calculated units are not VU but VU_B. By comparing the calculation values using wind speed units of "knot" and "m/s," the conversion relationship is found to be 1.00 VU = 0.136146 VU_B or 1.00VU_B = 7.345068VU [33] Based on the annual average values calculated using "knot" as the unit, FRYBERGER classified the wind dynamic environment for sand movement as follows: ≥400 VU is considered high wind energy, 200-399 VU is moderate wind energy, and <200 VU is low wind energy. Since wind speed is a vector, the sand drift potential in these 16 directions is combined to obtain the resultant sand drift potential (RDP) and resultant sand drift direction (RDD), which reflect the combined situation of sand drift potential. The ratio of RDP to DP is known as the wind direction variation index, which is also an important indicator reflecting the wind regime in the study area.

3. Results

3.1. Sand-Driving Wind

3.1.1. Sand-Driving Wind Regime in Different Seasons in Sandy Areas

Using wind speed and wind direction data from Shazhuyu and Guinan stations, the following analysis examines the sand-driving wind regime in the Talatan and Mugetan sandy areas according to different seasons. The maximum wind speed refers to the highest wind speed recorded during sand-driving events in each direction over the three-year period for each season. The average wind speed represents the mean wind speed of all sand-driving events in each direction over the three-year period for each season. The average frequency indicates the annual average number of sand-driving events in each direction during each season.

1). Spring Season

Based on wind speed and wind direction data from Shazhuyu and Guinan stations, a wind speed and direction map for sand-driving wind in spring is constructed, as shown in Figure 2.

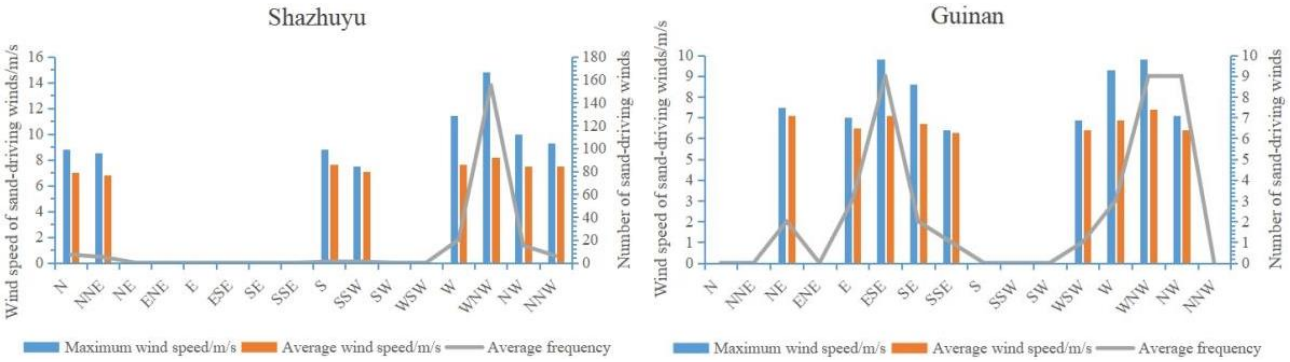

Figure 2. *Maximum wind speed, average wind speed and annual frequency of sand-driving wind at each position in spring.*

Observation at Shazhuyu Station revealed that there were 155 sand-driving wind events in the WNW direction, accounting for 75% of the total sand-driving wind events. The combined number of wind events in the W, WNW, and NW directions reached 190, representing 91% of the total. This suggests that the dominant wind direction in Talatan is WNW, followed by W and NW. On the other hand, Guinan Station observed 9 sand-driving wind events each in the WNW, NW, and ESE directions, accounting for 69% of the total. The combined number of wind events in the W, WNW, and NW directions made up 54% of the total, while those in the E, ESE, and SE directions accounted for 36%. This indicates that the primary wind directions in Mugetan are W, WNW, and NW, with secondary directions being E, ESE, and SE. The maximum wind speed and maximum value of average wind speed observed at Shazhuyu Station were 14.8m/s and 8.2m/s, respectively, both occurring in the WNW direction. For Guinan Station, the corresponding values in the primary WNW direction were 9.8m/s and 7.4m/s, while in the secondary ESE direction, they were 9.8m/s and 7.1m/s, respectively, These findings suggest that the main wind speeds in Talatan are also concentrated in the WNW direction, while in Mugetan, they are distributed in both the WNW and ESE directions.

2). Summer Season

Based on wind speed and wind direction data from Shazhuyu and Guinan stations, a wind speed and direction map for sand-driving wind in summer is constructed, as shown in Figure 3.

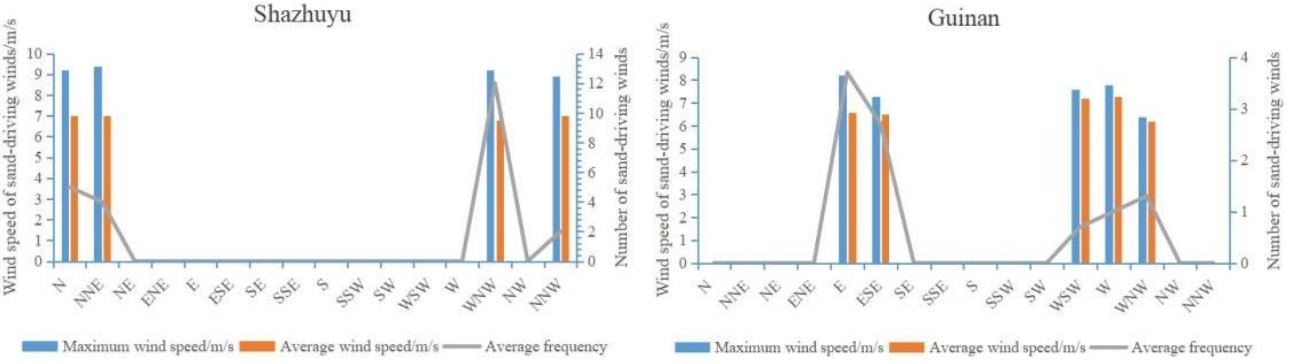

Figure 3. *Maximum wind speed, average wind speed and annual frequency of sand-driving wind at each position in summer.*

Observations at Shazhuyu Station revealed that there were 12 sand-driving wind events in the WNW direction, accounting for 52% of the total. The combined number of wind events in the N and NNE directions totaled 9, representing 39% of the total. This indicates that the dominant wind direction in Talatan is WNW, with secondary directions being N and NNE. On the other hand, Guinan Station observed 6.4 sand-driving wind events in the E and ESE directions, accounting for 68% of the total. The combined number of wind events in the WSW, W, and WNW directions made up 32% of the total. This suggests that the primary wind directions in Mugetan are E and ESE, with secondary directions being WSW, W, and WNW. The maximum wind speed and maximum value of average wind speed observed at Shazhuyu Station were 9.4m/s and 7.0m/s, respectively, both occurring in the NNE direction. However, the corresponding values were also recorded in the N and WNW directions, with speeds of 9.2m/s and 7.0m/s, indicating that wind speeds in the northern sector (N and NNE) are slightly higher than those in the Western sector (WNW). For Guinan Station, the maximum wind speed of 8.2m/s was recorded in the E direction, while the maximum value of average wind speed of 7.3m/s was observed in the W direction. However, there was not a significant difference in wind speeds between the primary and secondary wind directions.

3). Autumn Season

Based on wind speed and wind direction data from Shazhuyu and Guinan stations, a wind speed and direction map for sand-driving wind in autumn is constructed, as shown in Figure 4.

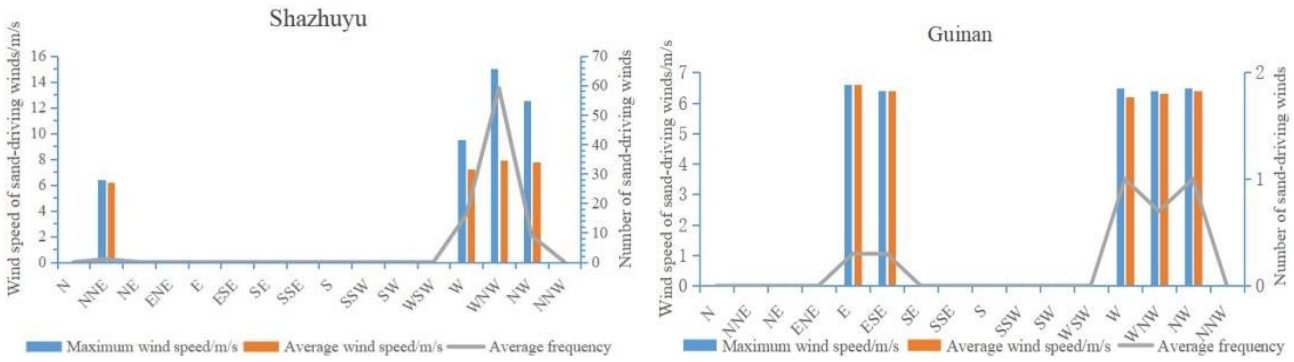

Figure 4. *Maximum wind speed, average wind speed and annual frequency of sand-driving wind at each position in autumn.*

Observations at Shazhuyu Station indicate that there were 59 sand-driving wind events in the WNW direction during autumn, accounting for 69% of the total. The combined number of wind events in the W, WNW, and NW directions reached 84, representing 99% of the total. This strongly suggests that the dominant wind direction in Talatan is WNW, followed by W and NW. On the other hand, Guinan Station recorded an annual average of 3.3 sand-driving wind events. Among these, 2.7 events occurred in the W, WNW, and NW directions, constituting 81% of the total. The remaining 19% were distributed in the E and ESE directions. This indicates that the primary wind directions in Mugetan are W, WNW, and NW, but the frequency of sand-driving wind is very low. The maximum wind speed and maximum value of average wind speed observed at Shazhuyu Station were 15.0m/s and 7.9m/s, respectively, both occurring in the WNW direction. For Guinan Station, the maximum wind speed was 6.6m/s, with a minimum of 6.4m/s. The maximum value of average wind speed was 6.6m/s, and the minimum was 6.2m/s. These findings suggest that Talatan experiences strong winds primarily in the WNW direction,, while Mugetan has a more varied wind pattern with less consistently strong winds. At Shazhuyu Station, the highest wind speed recorded was 15.0m/s, and the average wind speed was 7.9m/s, both occurring in the WNW direction. At Guinan Station, the highest wind speed was 6.6m/s, with the lowest recorded at 6.4m/s. The average wind speed had a high of 6.6m/s and a low of 6.2m/s. These findings suggest that Talatan experiences stronger winds primarily in the WNW direction.

4). Winter Season

Based on wind speed and wind direction data from Shazhuyu and Guinan stations, a wind speed and direction map for sand-driving wind in winter is constructed, as shown in Figure 5.

In the WNW direction of Shazhuyu, there were 115 sand-driving wind events, accounting for 75% of the total. The combined number of wind events in the W, WNW, and NW directions reached 153, representing 100% of the total.

This clearly indicates that the primary wind direction in Talatan is WNW, followed by W and NW. At Guinan Station, there were 7 sand-driving wind events in the W direction, accounting for 45% of the total. The combined number of wind events in the WNW, W, and WSW directions constituted 89% of the total, indicating that the primary wind directions in Mugetan are WNW, W, and WSW, with W being the most dominant. The maximum wind speed and maximum value of average wind speed at Shazhuyu were 14.0m/s and 8.0m/s, respectively, both occurring in the WNW direction. For

Guinan, the corresponding values in the primary wind direction were 8.7m/s and 7.0m/s, occurring in the W direction. From these observations, it can be concluded that the primary wind speed in Talatan is also located in the WNW direction, while it is in the W direction for Mugetan.

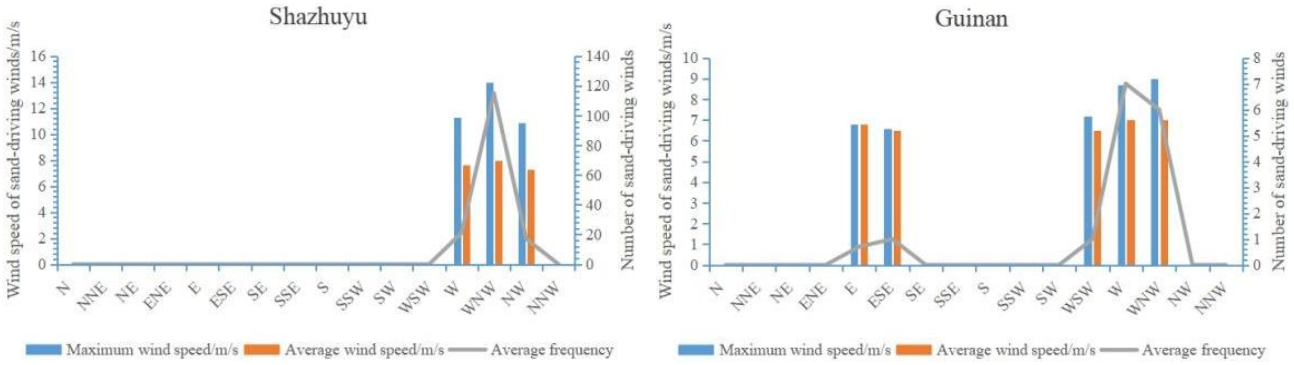

Figure 5. *Maximum wind speed, average wind speed and annual frequency of sand-driving wind at each position in winter.*

In summary, the primary wind direction in Talatan is WNW throughout the four seasons. Not only does the WNW direction have a significant advantage in the number of sand-driving wind events, but it also concentrates maximum wind speed and maximum value of average wind speed. On the other hand, Mugetan has distinct primary and secondary wind directions throughout the four seasons. The primary wind directions in spring, autumn, and winter are WNW, W, WSW, and NW, while the secondary directions are E and ESE. In summer, the situation is reversed. The maximum wind speed and maximum value of average wind speed are concentrated in the primary wind direction. Furthermore, based on the number of sand-driving wind events, Talatan has the highest frequency in spring (209 events) followed by winter (153 events), autumn (85 events), and summer (23 events). For Mugetan, the order is spring (39 events) > winter (15 events) > summer (9.4 events) > autumn (3.3 events). When considering the maximum value of average wind speed, Talatan has the highest values in spring (8.2m/s) followed by winter (8.0m/s), autumn (7.9m/s), and summer (7.0m/s). For Mugetan, the order is spring (7.4m/s) > summer (7.3m/s) > winter (7.0m/s) > autumn (6.6m/s).

3.1.2. Annual Sand-Driving Wind Regime in Sandy Areas

The period from June 2019 to May 2020 is designated as the 2019–2020 year, June 2020 to May 2021 as the 2020–2021 year, and June 2021 to May 2022 as the 2021–2022 year. The maximum wind speed refers to the highest wind speed recorded during all sand-driving wind events in that year. The average wind speed represents the mean wind speed of all sand-driving wind events in that year. The number of sand-driving wind events refers to the total count of such events in that year. The sand-driving wind frequency is calculated by dividing the number of sand-driving wind events by the total number of wind speed recordings in that year. Hourly data is used for the annual analysis, so the total number of wind speed recordings in a year is 8760.

Based on the sand-driving wind statistics from the Shazhuyu and Guinan meteorological stations, the following Table 1 is constructed:

Table 1. *Maximum wind speed and average wind speed of sand-driving wind in every year in Shazhuyu and Guinan (m/s).*

	Shazhuyu				Guinan			
	Maximum wind speed	Average wind speed	Number of sand-driving wind events	Sand-driving wind frequency	Maximum wind speed	Average wind speed	Number of sand-driving wind events	Sand-driving wind frequency
2019-2020	14.3	7.9	386	4.4%	9.3	6.8	66	0.75%
2020-2021	13.3	7.9	529	6.0%	9.0	6.6	73	0.83%
2021-2022	14.8	7.7	487	5.6%	9.8	7.1	61	0.70%
2019-2022	14.8	7.83	1402	5.3%	9.8	6.82	200	0.76%

Based on the table above, it can be observed that regardless of whether it's for each individual year or across all three years, the number of sand-driving wind events in Shazhuyu is approximately seven times that of Guinan. The maximum wind speed in Shazhuyu is approximately 5m/s higher than that in Guinan, while the average wind speed is approximately 1m/s higher. Overall, the wind speed in Talatan is significantly greater than that in Mugetan.

3.2. Sand Drift Potential

The following calculated values of sand drift potential represent the average for each direction over the course of three years for the respective season. Since wind energy below 200VU is considered low, the second decimal place of the sand drift potential value has a minimal impact on the classification of wind energy environments. To simplify calculations, sand drift potential values less than 0.01VU have been disregarded in the subsequent analysis.

3.2.1. Analysis by Season

1). Spring

Refer to Figure 6 for the sand drift potential in Talatan and Mugetan during the spring season.

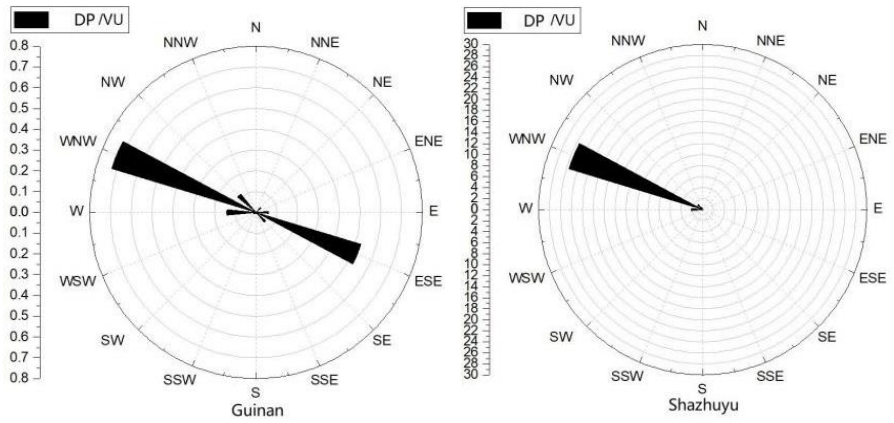

Figure 6. Rose plots of sand drift potentiall at each position in spring in Shazhuyu and Guinan.

In the spring season, in Talatan, the highest values were observed in the WNW direction with a maximum of 25.6VU, followed by 2.1VU in the W direction, and 1.3VU in the NW direction. The algebraic sum of sand drift potential in Talatan was 29.4VU, with the WNW direction contributing 87% of this total. In Mugetan, the maximum sand drift potential was 0.73VU in the WNW direction, with additional significant values of 0.53VU in the ESE direction, and lower values of 0.14VU and 0.12VU in the W and NW directions, respectively. The algebraic sum of sand drift potential in Mugetan was 1.70VU, with the WNW direction accounting for 43% and the ESE direction for 31% of the total.

2). Summer

Refer to Figure 7 for the sand drift potential in Talatan and Mugetan during the summer season.

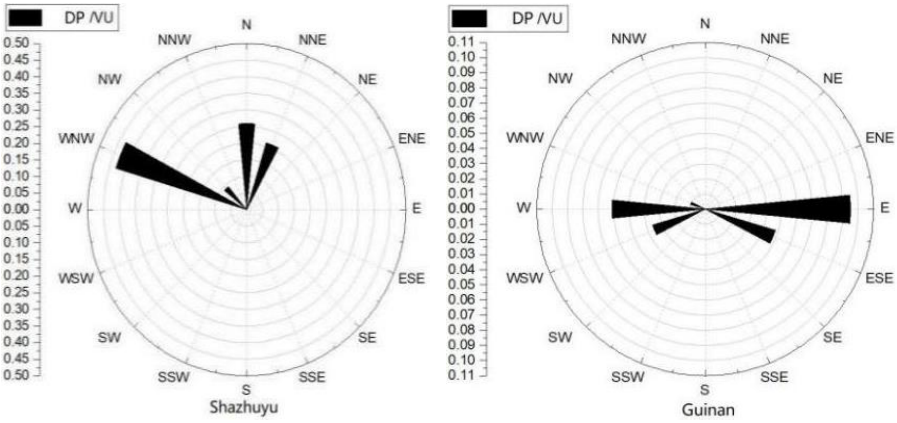

Figure 7. Rose plots of sand drift potentiall at each position in summer in Shazhuyu and Guinan.

In the summer season, all sand drift potential values for all directions in Talatan and Mugetan were less than 1.0VU. Only three sand drift potential values were ≥0.1VU, all of which were observed in Talatan. The maximum value was 0.43VU in the WNW direction, followed by 0.26VU and 0.21VU in the N and NNE directions, respectively. The maximum sand drift potential in Mugetan was 0.095VU in the E direction, followed by 0.061VU in the W direction. sand drift potential values for all other directions were less than 0.05VU. Additionally, the algebraic sum of sand drift potential in Talatan was 0.99VU, with the WNW direction contributing 43%, and the N and NNE directions combined contributing 47%. For Mugetan, the algebraic sum of sand drift potential was 0.25VU, with the E direction accounting for 38% and the W direction accounting for 24%.

3). Autumn

Refer to Figure 8 for the sand drift potential in Talatan and Mugetan during the autumn season.

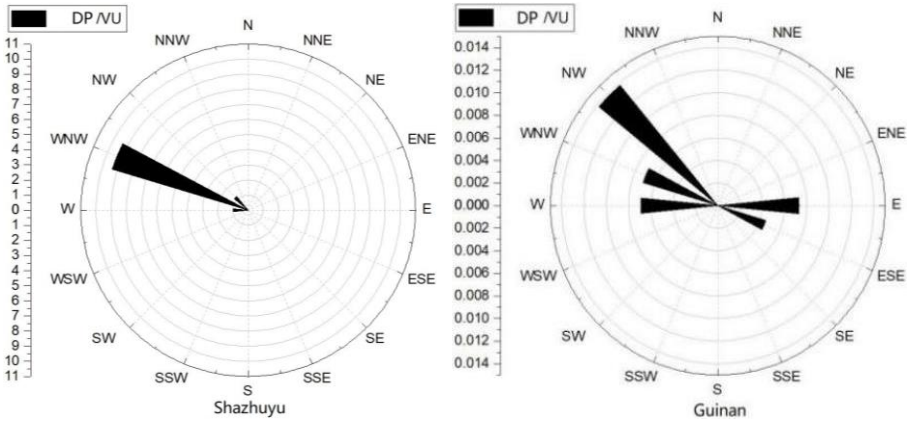

Figure 8. *Rose plots of sand drift potentiall at each position in autumn in Shazhuyu and Guinan.*

In the autumn season, there were only three sand drift potential values ≥1.0VU for each direction in Talatan and Mugetan, all of which were observed in Talatan. The maximum value was 9.3VU in the WNW direction, followed by 1.2VU and 1.0VU in the NW and W directions, respectively. The maximum sand drift potential in Mugetan was 0.014VU in the NW direction, followed by 0.0073VU in the E direction. sand drift potential values for all other directions were less than 0.007VU. Additionally, the algebraic sum of sand drift potential in Talatan was 11.5VU, with the WNW direction contributing 81% of the total, and the NW and W directions combined contributing 19%. For Mugetan, the algebraic sum of sand drift potential was 0.039VU, with the NW direction accounting for 36% and the E direction accounting for 19%.

4). Winter

Refer to Figure 9 for the sand drift potential in Talatan and Mugetan during the winter season.

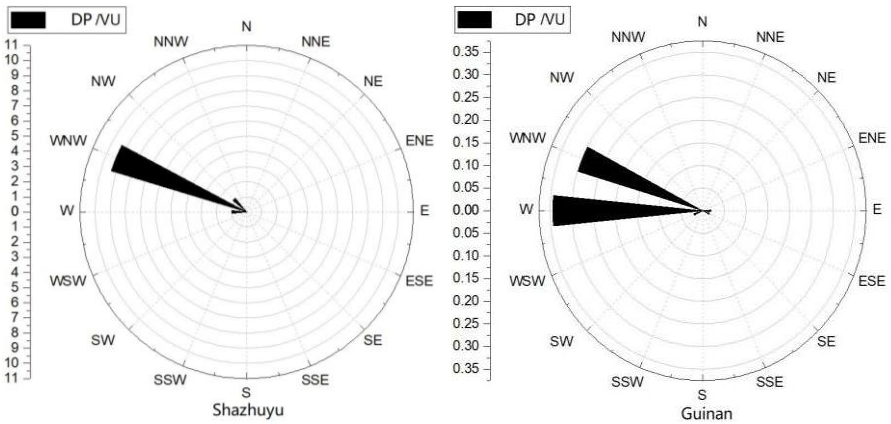

Figure 9. *Rose plots of sand drift potentiall at each position in winter in Shazhuyu and Guinan.*

During the winter, In Talatan, the maximum value was 17.2VU in the WNW direction, followed by 2.2VU and

1.2VU in the W and NW directions, respectively. The maximum sand transport potential value of Mugetan was 0.34VU in the W direction, followed by 0.30VU in the WNW direction. The sand transport potential values in other directions were all less than 0.03VU. Secondly, the algebraic sum of sand transport potential in Talatan was 20.5VU, with 84% of the total coming from the WNW direction, and 16% from the NW and W directions. The algebraic sum of sand transport potential in Mugetan was 0.70VU, with 49% of the total coming from the W direction and 43% from the WNW direction.

3.2.2. General Analysis of the Sandy Area

Please see the following Table 2 for the sand transport potential of Talatan and Mugetan in the four seasons.

Table 2. Sand drift potential in every season in Shazhuyu and Guinan.

	Shazhuyu				Guinan			
	DP (VU)	Main sand drift direction	Main sand drift direction DP (VU)	Proportion of DP in the main sand drift direction	DP (VU)	Main sand drift direction	Main sand drift direction DP (VU)	Proportion of DP in the main sand drift direction
spring	29.4	WNW	25.6	87%	1.70	WNW	0.73	43%
summer	0.99	WNW	0.43	43%	0.25	E	0.095	38%
autumn	11.5	WNW	9.3	81%	0.039	NW	0.014	36%
winter	20.5	WNW	17.2	84%	0.70	W	0.34	49%

Based on the table provided, it is evident that the dominant sand drift direction in Talatan is highly consistent, primarily in the WNW direction, accounting for a significant proportion of the total, exceeding 80% in three seasons except for summer, where it is 43%. In contrast, the dominant sand drift directions in Mugetan are more diverse, with the western direction being the primary one in spring, autumn, and winter, averaging 43%. However, in summer, the dominant direction shifts to the east. When comparing the seasonal variations in sand drift potential, Talatan exhibits a clear pattern with spring being the highest, followed by winter, Autumn, and Summer. The differences are pronounced, forming an arithmetic sequence with a common difference of approximately 10VU. On the other hand, Mugetan also shows significant seasonal variations, with spring being the highest, followed by Winter, Summer, and Autumn. Notably, the difference between Autumn and Spring is the most significant, with Autumn's sand drift potential being only 2% of Spring's, and Summer being 15% of Spring's. Unlike Talatan, the order of Summer and Autumn is reversed in Mugetan.

3.3. Resultant Sand Drift Potential, Resultant Sand Drift Direction, and Wind Direction Variability Index

The resultant sand drift potential (RDP), resultant sand drift Direction (RDD), and Wind Direction Variability Index (RDP/DP) for Talatan and Mugetan were calculated based on the aeolian data. These values are presented in Table 3 below.

Table 3. DP (VU), RDP (VU), RDD and RDP / DP in every season in Shazhuyu and Guinan.

	Shazhuyu				Guinan			
	DP	RDP	RDP /DP	RDD	DP	RDP	RDP /DP	RDD
spring	29.4	29.0	99%	WNW	1.70	0.32	19%	WNW
summer	0.99	0.78	97%	NNW	0.25	0.046	18%	SE
autumn	11.5	11.4	99%	WNW	0.039	0.016	41%	NW
winter	20.5	20.3	99%	WNW	0.70	0.61	87%	W
All year round	62.39	61.48	99%	WNW	2.689	0.89	33%	W

Based on Table 3, the resultant sand drift Direction (RDD) for Talatan remains consistently WNW throughout the four seasons and the annual average, indicating a predominantly unidirectional sand drift. In contrast, the RDD for Mugetan varies significantly across the seasons, but predominantly remains westward except for summer. The annual RDD for Mugetan is also westward. In terms of the annual sand drift potential, both Talatan and Mugetan exhibit values less than 200 VU, indicating a low-wind energy environment. Notably, the annual sand drift potential for Mugetan is particularly low, amounting to only 2.689 VU, which is 4.3% of Talatan's value. Talatan exhibits a very high index, with values close to 0.99 for all seasons except summer (0.97), indicating a narrow and unidirectional wind regime. In contrast, Mugetan experiences more variable wind regime, with the index ranging from a low of 0.18 in summer to a high of 0.87 in winter. The annual average index for Mugetan is 0.33, indicating more variable wind directions compared to Talatan. Combined with the sand drift rose diagrams, we can classify the wind regime as follows: Talatan exhibits a narrow single-peak wind regime, while Mugetan has a compound wind regime in spring and summer, a blunt double-peak wind regime in autumn, and a sharp double-peak wind regime in winter.

4. Discussion

4.1. Comparative Analysis of Wind Regime in the Gonghe Basin

Chen Zongyan et al. [22] utilized wind data from Chaka, Gonghe, and Guinan stations between 2012 and 2015 to analyze the wind-blown sand environment in the Gonghe Basin (hereinafter referred to as the 2018 article). Additionally, they used wind data from these three stations between 1971 and 2015 to analyze the wind characteristics and trends in the basin [23] (hereinafter referred to as the 2020 article). This study uses data from Shazhuyu and Guinan stations from June 2019 to May 2022. The results show that the dominant wind direction and average wind speed of the sand-driving wind at Guinan Station, as well as the sand drift potential in spring, summer, and autumn, are similar to those reported in the 2018 article. However, there are significant differences in the RDP and DP values for winter. The 2018 article reported values of 7.0 VU and 6.6 VU, respectively, while this study found values of 0.70 VU and 0.61 VU. This suggests that while there has been little change in the wind speed and direction of the sand-driving wind at Guinan from 2012 to 2022, the decrease in winter sand drift potential may be due to a reduction in the frequency of sand-driving wind events.The 2020 article analyzed the DP and RDP at Guinan from the 1970s to the 2000s, finding values of 68.30, 21.00, 6.90, 3.80 VU and 52.50, 13.60, 5.50, 2.20 VU, respectively, showing a decreasing trend with narrowing amplitudes. This study calculates the DP and RDP for the first three years of the 2020s as 2.69 VU and 0.89 VU, respectively, which is consistent with and continues this trend.

On the Qinghai-Tibet Plateau, the eastern sandy area of Qinghai Lake Located in the northern part of the study area is separated by the Qinghai South Mountain. According to research [26], the sand-driving winds in the eastern sandy area of Qinghai Lake in March, April, and May of 2006, 2009, 2012, and 2015 were dominated by the west wind group, with DP mainly in the directions of W, WNW, WSW, and SW. The annual DP values were less than 200 VU, indicating a low-wind-energy region with either a single-peak or narrow double-peak wind condition.The Wulan County, situated in the east of the Qaidam Basin, borders the western end of the Gonghe Basin. Studies [20] show that the primary and secondary wind directions in Wulan during spring are WSW and NNE, respectively, with an annual DP of 34.0 VU, classifying it as a low-wind-energy region with a blunt double-peak wind regime.Both the eastern sand area of Qinghai Lake and Wulan County belong to low-wind-energy regions. The sand-driving winds in spring are predominantly from the west wind group in all three locations, albeit with variations in wind regime. Specifically, the eastern sandy area of Qinghai Lake exhibits a single-peak or narrow double-peak wind condition, similar to that of Talatan, while Mugetan presents a compound wind regime during spring. Wulan County falls somewhere in between, with a blunt double-peak wind regime. In summary, the characteristics of sand-driving winds and DP in the sandy areas on both sides of Longyang Gorge, as well as in the eastern sandy area of Qinghai Lake to the north and Wulan County to the west, are relatively similar.

While the dominant wind direction at Mugetan is the westerly group, there are still easterly sand-driving wind present in all four seasons. Due to the very low sand drift potential, despite the abundance of sand sources, wind-blown sand into the reservoir is not severe. In contrast, the sand-driving wind and sand drift potential at Talatan are both relatively high, with a predominantly WNW wind direction and a high wind direction variability index. In addition, there are abundant sand sources and a flat terrain at Talatan and the northwest shore of Longyangxia Reservoir. Therefore, the wind-blown sand at Talatan poses a significant hazard to Longyangxia Reservoir. When addressing the issues at the two sites, the focus should be on Talatan. In addition to traditional methods such as sealing sand areas, planting vegetation, and setting up grass squares, actively building photovoltaic bases is also a good measure for sand control.

4.2. Analysis of the Causes of Wind Regime Differences Between Talatan and Mugetan

Many scholars [34-36] have analyzed the wind regime and influencing factors of the Gonghe Basin as a whole, with

relatively little research on the differences in wind speed and direction between the two sites in the southeastern part of the basin. Factors that affect wind speed and direction typically include Earth's rotation, the Coriolis force, temperature differences between land and ocean, seasonal factors, terrain, temperature, precipitation, and horizontal pressure gradient force [37-43] Since the straight-line distance between Shazhuyu Station and Guinan Station is approximately 90 km, the effects of Earth's rotation, the Coriolis force, and temperature differences between land and ocean can be neglected. Since we are comparing sand-driving wind in the same season, seasonal factors are also not considered. The reasons for the significantly higher maximum wind speed, average wind speed, frequency, seasonal sand drift potential, and annual sand drift potential at Talatan compared to Mugetan can be attributed to the following three factors:

Terrain: Gonghe Basin generally trends in the WSW-ESE direction, with a narrow width in the west and a wide width in the east, resembling a gourd shape. In the west, it is connected to the Qaidam Basin, and in the east, it reaches the Xiqing Mountain of the Qinling Mountains. The east-west length axis of the basin is approximately 300 kilometers. The north-south direction is the narrowest at the westernmost end of the basin, at about 30 kilometers, and the widest at the left bank of the Longyang Gorge, at about 90 kilometers. When the atmospheric circulation of the Qaidam Basin enters the Gonghe Basin, the wind speed gradually decreases due to the basin's gradual widening from north to south. Additionally, due to the orientation of the basin, the wind direction in Shazhuyu is almost entirely WSW. After the westerly wind passes through Shazhuyu, the degree of widening in the north-south direction of the basin intensifies, forming a "horn effect," which causes air expansion, pressure reduction, and gradual weakening of the wind speed. After crossing the Longyang Gorge Reservoir, it is further blocked by the Chanashan on the right bank of the reservoir, causing the wind speed entering Mugetan to decrease again.

Precipitation: From June 2019 to May 2022, there were 27 months where the monthly precipitation at the Guinan Station was greater than that at the Shazhuyu Station, with an average difference of 19.8mm. Only 9 months had lower precipitation at the Guinan Station, with an average difference of 4.6mm lower. This indicates that precipitation suppresses wind speed and the frequency of sand-driving wind.

Wind direction stability: The wind direction in Talatan is much more stable compared to Mugetan. When the wind direction is relatively stable, air flow forms a relatively consistent and continuous airflow channel. In this situation, the wind speed may be relatively high, as a stable wind direction facilitates the continuation and strengthening of air flow, reducing energy dissipation and turbulence generation. The above analysis is qualitative, and further quantitative research is needed for specific quantification.

5. Conclusions

The dominant wind direction for Talatan is WNW across all four seasons, while Mugetan experiences westerly winds during spring, autumn, and winter, shifting to easterly winds in summer. Both areas exhibit their highest wind speeds in their respective dominant wind directions. When assessing wind energy based on sand-driving wind frequency, average wind speed, and maximum wind speed, Talatan ranks as follows: spring > winter > autumn > summer. Mugetan's ranking is: spring > winter > summer > autumn. Talatan experiences approximately seven times as many sand-driving wind events as Mugetan, with its maximum wind speeds being approximately 5m/s higher and average wind speeds around 1m/s higher than those in Mugetan." Both Talatan and Mugetan have annual sand drift potentials less than 200VU, indicating low wind energy environments, but the annual average sand drift potential for Talatan is 23 times higher than that of Mugetan. Talatan has a very high wind direction variability index, exhibiting a narrow single-peak wind regime. Mugetan, on the other hand, experiences a wider range of wind direction variability indices, with compound wind regime during spring and summer, a blunt double-peak in autumn, and a sharp double-peak in winter. The significant differences in sand-driving wind regime between Talatan and Mugetan are primarily attributed to differences in terrain, precipitation, wind direction stability.

When formulating the wind-sand control plan for Longyangxia Reservoir, it is necessary to comprehensively consider the seasonal distribution of wind speed, wind direction, and sand drift potential in Talatan and Mugetan. The primary focus should be on preventing and controlling the wind-sand brought by the west wind in spring. Furthermore, the fact that the annual sand drift potential of Talatan is significantly higher than that of Mugetan underscores the importance of considering local meteorological differences when assessing the feasibility of wind energy projects. Attributing these differences to factors such as terrain, precipitation, and wind direction stability emphasizes the interdisciplinary nature of wind energy research, which is crucial for comprehensively understanding the interactions between environmental factors and their impact on the quality of wind energy resources.

Abbreviations

WNW	West Northwest
N	North
NNE	North North East
NE	Northeast
ENE	East Northeast
E	East
ESE	East Southeast
SE	Southeast
SSE	South South East
S	South

SSW	South South West
SW	Southwest
WSW	West Southwest
W	West
NW	Northwest
NNW	North North West
DP	Sand Drift Potential
RDP	Resultant Sand Drift Potential
RDD	Resultant Sand Drift Direction
VU	Vector Units

Acknowledgments

The authors would like to acknowledge to all reviewers who have given us valuable information.

Author Contributions

Lechun Zhang: Conceptualization, Data curation, Formal Analysis, Writing—original draft

Dengshan Zhang: Supervision, Writing—review & editing

Guoyuan Xu: Data curation

Fengling Dong: Visualization

Wanbing Tuo: Funding acquisition

Data Availability Statement

Not applicable.

Funding

This work is supported by the National Natural Science Foundation of China (Grant number: 41661001); Research and Development of Key Technologies and Integrated Demonstration of Comprehensive Sand Prevention and Control in Alpine Sandy Areas of Hainan Prefecture, Qinghai Province;Qinghai Institute of Technology 'Kunlun Yingcai' Talents Introduction of Scientific Research" Project (2023-QLGKLYCZX-25).

Conflicts of Interest

The authors declare no conflict of interest.

References

[1] Ma, H.; Xiao, F.; Dong, Z., Dynamics and driving factors of land desertification in Gonghe County, Qinghai Province from 2000 to 2020. Journal of Arid Land Resources and Environment 2022, 36, 139-148. https://doi.org/10.13448/j.cnki.jalre.2022.157

[2] Sha, Z.; Zeng, Y.; Ma, H., Dynamic study on land desertification in Longyangxia reservoir area supported by remote sensing and GIS. Journal of Desert Research 2000, 20, 51-54. https://doi.org/10.3321/j.issn:1000-694X.2000.01.010

[3] Li, F.; Tang, H.; Su, W., Remote sensing monitoring of desertification in Longyangxia Reservoir Area of Qinghai Province. Journal of Desert Research 2003, 23, 686-690. https://doi.org/10.3321/j.issn:1000-694X.2003.06.017

[4] Li, S.; Yan, C, Z.; Song, X., Remote sensing monitoring of desertification on the two sides of Longyangxia Reservoir in recent 30 years. Journal of Desert Research, 2011, 31, 836-841.

[5] Duan, Q.; Shi, M.; Wang, B., Present situation of sandstorm in Longyangxia reservoir area and its influence on the reservoir area. Arid Zone Research 1990, 3, 22-29. https://doi.org/10.13866/j.azr.1990.03.004

[6] Hu, M.; Li, X.; Zuo, H., Dynamics of land desertification in Guinan County, Gonghe Basin from 1989 to 2014. Journal of Desert Research 2018, 38, 30-38. https://doi.org/10.7522/j.issn.1000-694X.2016.00130

[7] Shao, M.; Luo, W.; Che, X., Characteristics of sandstorm transport and estimation of potential inflow in Longyangxia reservoir area from 1987 to 2019 based on COSI-CORR technology. Journal of Desert Research 2021, 41, 249-261. https://doi.org/10.7522/j.issn.1000-694X.2021.00154

[8] Dong, G.; Gao, S.; Jin, J., Land desertification and its control in Gonghe Basin of Qinghai Province. Journal of Desert Research 1989, 9, 61-75.

[9] Zhang, D., Quantitative analysis of influencing factors of land desertification in Gonghe Basin of Qinghai. Journal of Desert Research 2000, 20, 59-62. https://doi.org/10.3321/j.issn:1000-694X.2000.01.012

[10] Wu, Z., Wind-blown sand landform and sand control engineering. 2nd ed.; Science Press: Beijing, China, 2003; 385-390.

[11] Li, J.; Su, Z.; Hu, G., Common indexes for judging the intensity of sandstorm activity and their application. Journal of Desert Research 2010, 30, 788-794.

[12] Wang, Z.; Niu, G.; Liu, B., Comparison and applicability analysis of three estimation indexes of sandstorm activity intensity. Journal of Desert Research 2021, 41, 118-126. https://doi.org/10.7522/j.issn.1000-694X.2021.00030

[13] Zu, R.; Zhang, K.; Qu, J., Study on wind characteristics in Taklimakan desert. Arid Land Geography 2005, 28, 167-170. https://doi.org/10.3321/j.issn:1000-6060.2005.02.006

[14] Mao, D.; Cai, F.; Lei, J., Characteristics of aeolian sand activities in the southern margin of Taklimakan Desert in the lower reaches of Qira River in Xinjiang. Journal of Arid Land Resources and Environment 2016, 30, 169-174. https://doi.org/10.13448/j.cnki.jalre.2016.23

[15] Liu, T.; Yang, X; Dong, J., A preliminary study of relation between megadune shape and wind regime in the Badain Jaran Desert. Journal of Desert Research 2010, 30, 1285-1291.

[16] Pang, Y.; Wu, B.; Jia, X., Characteristics of wind regime and sand drift potential in Mu Us sandy land. Journal of Desert Research 2019, 39, 62-67. https://doi.org/10.7522/j.issn.1000-694X.2018.00024

[17] Gu, L.; Lv, P.; Ma, F., Characteristics of wind regime and sand drift potential in Mu Us sandy land under different data sources. Journal of Desert Research 2022, 42, 54-62 https://doi.org/10.7522/j.issn.1000-694X.2022.00014

[18] Luo, F.; Gao, J.; Xin, Z., Characteristics of sand-driving wind regime and sediment transport in northeast edge of Ulan Buh Desert [J]. Transactions of the Chinese Society of Agricultural Engineering (Transactions of the CSAE), 2019, 35(4): 145－152. (in Chinese with English abstract) https://doi.org/10.11975/j.issn.1002-6819.2019.04.018

[19] Yang, Y.; Lv, P.; Ma, F., Influence of wind regime in the southwest of Ulan Buh Desert on the formation of dome dunes. Journal of Desert Research 2021, 41, 19-26. https://doi.org/10.7522/j.issn.1000-694X.2020.00120

[20] Chen, Z.; Dong, Z.; Wang, Q., Characteristics of wind regime and sand drift potential in Qaidam Basin. Journal of Desert Research, 2020, 40, 195-203. https://doi.org/10.7522/j.issn.1000-694X.2019.00090

[21] Hu, G.; Dong, Z.; Zhang, Z., Characteristics of wind regime and sand transport potential in Zoige Basin. Journal of Desert Research 2020, 40, 20-24. https://doi.org/10.7522/j.issn.1000-694X.2020.00044

[22] Chen, Z.; Dong, Z.; Wang, Q. Wind regime and aeolian landform in Gonghe Basin, Qinghai. Journal of Desert Research 2018, 38, 492-499. https://doi.org/10.7522/j.issn.1000-694X.2017.00014

[23] Chen, Z.; Dong, Z.; E, C., Characteristics and changing trend of wind regime in Gonghe Basin from 1971 to 2015. Journal of Lanzhou University (Natural Science Edition) 2020, 56, 224-231. https://doi.org/10.13885/j.issn.0455-2059.2020.02.011

[24] Li, J.; Han, L.; Zhao, Y., Wind regime and sand drift potential in desertification areas in northern Shanxi. Journal of Desert Research 2016, 36, 911-917. https://doi.org/10.7522/j.issn.1000-694X.2015.00236

[25] Liang, X.; Niu, Q.; An, Z., Characteristics of sand wind and sand transport potential in Yadan landform area south of Suoyang City, Guazhou, Gansu Province. Journal of Desert Research 2019, 39, 48-55. https://doi.org/10.7522/j.issn.1000-694X.2018.00079

[26] Zhang, L.; Zhang, D.;Wang, H., Characteristics of sand-driving wind regime and sand drift potential in windy season in the east sandy area of Qinghai Lake. Journal of Desert Research 2023, 37, 91-977. https://doi.org/10.13448/j.cnki.jalre. 2023. 066

[27] Amy, L. E.; Leslie, D. M.; Joseph. A. M.; Shannon. A. M, Late Quaternary Soil Development Enhances Aeolian Landform Stability, Moenkopi Plateau, Southern Colorado Plateau, USA. Geosciences 2018, 8, 146-164. https://doi.org/10.3390/geosciences8050146

[28] Xie, S.; Qu, J.; Han, Q.; Pang, Y., Wind dynamic environment and wind tunnel simulation experiment of bridge sand damage in Xierong section of Lhasa–Linzhi Railway. Sustainability 2020, 12, 5689. https://doi.org/10.3390/su12145689

[29] Rahdari, M. R.; Rodr ́guez-Seijo, A. Monitoring Sand Drift Potential and Sand Dune Mobility over the Last Three Decades (Khartouran Erg, Sabzevar, NE Iran). Sustainability 2021, 13, 9050. https://doi.org/10.3390/SU13169050

[30] Fryberger, S. G.; Dean, G. Dune forms and wind regime. In: McKee, E. D. (Ed.), A study of global sandy seas. Washington: United States Government Printing Office, 1979; 137-169.

[31] Sun, X.; Fang, Y.; Zhao, J., Temporal and spatial distribution characteristics of sand drift potential in Taklimakan Desert. Arid Land Geography 2020, 43, 38-46. https://doi.org/10.12118/j.issn.1000-6060.2020.01.05

[32] Fang, Y.; Zhao, J.; Guo, Y., Fryberger's calculation method of sand drift potential and deviation analysis of its estimated value - taking Taklimakan desert as an example. Arid Land Geography 2015, 38, 95-102. https://doi.org/10.13826/j.cnki.cn65-1103/x.2015.01.013

[33] Bullard, J. E., A note on the use of the "Fryberger method" for evaluating potential sandy transport by wind. Journal of Sediment Research 1997, 67, 499-501. https://doi.org/10.1306/d42685a9-2b26-11d7-8648000102c1865d

[34] Zhang, D.; Ga, S.; Shi, M., Land desertification and its control in Qinghai Plateau. 1st ed.; Science Press: Beijing, China, 2009; 39-96.

[35] Xu, S.; Xu D.; Shi S., Aeolian sand accumulation in Gonghe Basin, Qinghai Province. Journal of Desert Research 1982, 2, 1-8.

[36] Liu, J.; Chen, B.; Xu, D., Study on formation mechanism of wind energy resources in Gonghe Basin, Qinghai Province. Northwest Hydropower. 2022, 6, 144-149. https://doi.org/10.3969/j.issn.1006-2610.2022.06.024

[37] Souza Ferreira, G. W.; Reboita, M. S.; Ribeiro, J. G. M.; Carvalho, V. S. B.; Santiago, M. E. V.; Silva, P.; Baldoni, T. C.; de Souza, C. A., Assessment of the Wind Power Density over South America Simulated by CMIP6 Models in the Present and Future Climate. Climate 2023, 62, 1729–1763. https://doi.org/10.1007/S00382-023-06993-3

[38] ElSayed, H.; Omar, A.; Abdullah, A.; Abdoul, J, N., Characterisation of Sand Accumulations in Wadi Fatmah and Wadi Ash Shumaysi, KSA, Using Multi-Source Remote Sensing Imagery. Remote Sensing 2019, 11, 2824-2841. https://doi.org/ 10.1007/S00382-023-06993-3

[39] Ma, X.; Li, Y.; Li, Z., The Projection of Canadian Wind Energy Potential in Future Scenarios Using a Convection-Permitting Regional Climate Model. Energy 2022, 8, 7176–7187. https://doi.org/10.1016/J.EGYR.2022.05.122

[40] Rusu, E., An Evaluation of the Wind Energy Dynamics in the Baltic Sea, Past and Future Projections. Energy 2020, 160, 350–362. https://doi.org/10.1016/j.renene.2020.06.152

[41] Rusu, E., Assessment of the Wind Power Dynamics in the North Sea under Climate Change Conditions. Energy 2022, 195, 466–475. https://doi.org/10.1016/j.renene.2022.06.048

[42] Yang, Y.; Javanroodi, K.; Nik, V. M., Climate Change and Renewable Energy Generation in Europe—Long-Term Impact Assessmenton Solar and Wind Energy Using High-Resolution Future Climate Data and Considering Climate Uncertainties. Energy 2022, 15, 302. https://doi.org/10.1007/s11433-010-0148-4

[43] Costoya, X.; Castro, M.; Carvalho, D.; Feng, Z.; Gómez-Gesteira, M., Climate Change Impacts on the Future Offshore Wind Energy Resource in China. Energy 2021, 175, 731–747. https://doi.org/10.1016/j.renene.2021.05.001

Biography

Lechun Zhang obtained his master's degree in Geodesy and Surveying Engineering from China University of Geosciences (Beijing) in 2008. From then to 2024, he has been working as a teacher in Qinghai University. Now he is also pursuing his doctorate degree at Qinghai University. He has participated in multiple domestic research projects, and moreover, he holds a certificate as a registered surveyor.

Research Field

Lechun Zhang: Geodesy, Surveying Engineering, Remoting Sence, Ecological Environment Research in Arid Areas, Combating Desertification